Electronic Supplementary Material (ESI) for Journal of Materials Chemistry A.

Supporting Information

Discharging antibonding orbital electrons of 1T-MoS_2 by S-rich treatment for promoting photocatalytic H_2 evolution

Pinsi Deng,‡[a] Duoduo Gao,‡[a] Ping Wang,*[a] Xuefei Wang,[a] Feng Chen[a] and Huogen Yu*[a,b]

[a] School of Chemistry, Chemical Engineering and Life Sciences, Wuhan University of Technology, Wuhan 430070, PR China

[b] Laboratory of Solar Fuel, Faculty of Materials Science and Chemistry, China University of Geosciences, Wuhan, 430074, PR China

‡ These authors contributed equally to this work.

*Corresponding authors. Tel: +86(27)87749379;

E-mail: wangping0904@whut.edu.cn (Ping Wang);

huogenyu@163.com (Huogen Yu)

SI Experimental

SI-1 Materials

Sodium molybdate dihydrate (Na_2MoO_4•$2H_2O$), hydrazine hydrate (N_2H_4•H_2O, 85 wt%), sulfur (S), thiourea (CH_4N_2S), cadmium nitrate tetrahydrate ($Cd(NO_3)_2\cdot 4H_2O$), sodium sulfide nonahydrate ($Na_2S\cdot 9H_2O$), ethanol (C_2H_5OH), lactic acid ($C_3H_6O_3$), triethanolamine ($C_6H_{15}NO_3$), and melamine ($C_3H_6N_6$) were of analytical grade from Shanghai Chemical Reagent Ltd. (PR China). The titanium dioxide (TiO_2) were commercial TiO_2 (P25) from Degussa (Germany). The above materials were used without further purification.

SI-2 Characterization

The transmission electron microscope (TEM) (JEM-2100F, JEOL, Japan), X-ray diffraction (XRD) (Rigaku, D/MX-IIIA, Japan), Raman (Invia, Renishaw, UK), X-ray photoelectron spectroscopy (XPS) (Thermo Fisher, Escalab 250Xi, USA), in-situ irradiated XPS spectroscopy (Thermo Escalab 250Xi instrument with Al K α X-ray radiation, USA)，UV-vis spectrophotometer (UV-2450, Shimadzu, Japan), were used to confirm the microstructures of the as-prepared samples. Steady-state photoluminescence (PL) spectra were achieved by F-7000 fluorescence spectrophotometer (Japan, Hitachi). Time-resolved PL spectra were researched via a FLS920 fluorescence lifetime spectrophotometer (Edinburgh Instruments, UK).

SI-3 Photocatalytic H_2-evolution measurement

The photocatalytic H_2-evolution activity was measured in line with previous work. In brief, 50 mg of the prepared photocatalysts were added into ethanol aqueous solution (80 mL, 25 vol%) as sacrificial agent in a Pyrex glass reaction cell under sonication. The above suspension was purged with nitrogen for 15 min to remove extra gases, then directly radiated by four LED lights (3 W, 365 nm) to generate H_2. When the increase of generated H_2 tended to be steady, 400 μL of generated hydrogen was analyzed via a gas chromatograph (Shimadzu, GC-2014C, Japan) with a thermal conductivity detector and a 0.5 nm molecular sieve column regular every half hour intervals. For the cycling tests, the above system was re-bubbled with N_2 to evaluate the produced amount of H_2 and photocatalyst was recycled for the next H_2-generation measurement. The apparent quantum efficiencies (AQE) were calculated via the following equation:

$$\mathrm{AQE}(\%)=\frac{\text{number of reacted eletrons}}{\text{number of incident photons}}\times 100$$
$$=\frac{\text{number of evolved } \mathrm{H}_2 \text{ molecules}\times 2}{\text{number of incident photons}}\times 100$$
$$=\frac{2R_{\mathrm{H}_2}t_1N_A}{EAt_2\lambda/hc}=6.6482\times 10^{-5}\times R_{\mathrm{H}_2}/(E\times A\times\lambda)$$

R_{H_2} (μmol h^{-1}) represents the H_2 evolution rate, E (W cm^{-2}) represents the monochromatic light intensity, A (cm^2) represents the light radiation area of the reaction system, λ (m) represents the monochromatic wavelength, while t_1 (h), t_2 (s), h (W), and c (m s^{-1}) are constants with values of 1, 3600, 6.626×10^{-34} and 3×10^8, respectively. In this work, 50 mg of the photocatalyst was irradiated by four 365 nm-LED lights as the light source. The light radiation area (A) and the light intensity (E)

of the reaction system are 1 × 4 cm^2 and 80 mW cm^{-2}, respectively. R_{H_2} is obtained through the measurement of gas chromatograph and subsequent calculations.

SI-4 DFT calculations

The density functional theory (DFT) calculations were carried out by using the Vienna Ab initio Simulation Package (VASP). The exchange–correlation interaction was described by generalized gradient approximation (GGA) with the Perdew–Burke–Ernzerhof (PBE) functional. The energy cutoff and Monkhorst–Pack k-point mesh were set as 450 eV and 3 × 3 × 1, respectively. The convergence threshold was set as 10^{-5} eV for energy and 0.01 eV $Å^{-1}$ for force. For the construction of surface models, a vacuum of 20 Å was used to ensure that no appreciable interaction occurred between periodic structures. The Gibbs free energy of H atom adsorption (ΔG_{H*}) was defined as $\Delta G_{H*} = \Delta E_{H*} + \Delta E_{ZPE} - T\Delta S_H$. The entropy of H_2 gas at 298 K is 130 J mol^{-1} K^{-1}. Therefore, $T\Delta S_H$ was calculated to be –0.20 eV. In this case, one Mo atom is removed from original 1T-MoS_2 and/or an additional S atom is attached to the S of 1T-MoS_2 for simulating the S-rich structure of 1T-MoS_{2+x}.

SI-5 Photoelectrochemical measurements

The photoelectrochemical test was carried out via an electrochemical workstation (CHI660E, Chenhua Instrument, China) in a typical three-electrode system, which equipped with the electrolyte solution (0.5 mol L^{-1} Na_2SO_4 solution), counter electrode (platinum electrode), reference electrode (saturated Ag/AgCl electrode) and working electrode (fluorine-doped tin oxide (FTO) glass coated with photocatalysts). The linear sweep voltammetry (LSV) curves were measured at the potential ranging from −0.8 to −1.4 V (*vs* Ag/AgCl) with a scan rate of 10 mV s^{-1}. The transient photocurrent responses with time (*i-t* curve) can be achieved at a bias potential of +0.5 V during repeated On/Off illumination cycles. The electrochemical impedance spectroscopy (EIS) was carried out in the frequency range of 0.001 Hz-10^6 Hz with an ac amplitude of 10 mV at the open circuit voltage.

SI-6 Synthesis and photocatalytic H_2-evolution measurement of 1T-MoS_{2+x}/CdS and 1T-MoS_{2+x}/g-C_3N_4

The 1T-MoS_{2+x}/CdS and 1T-MoS_{2+x}/g-C_3N_4 photocatalyst can be obtained by the similar procedure as the 1T-MoS_{2+x}/TiO_2 via employing CdS and g-C_3N_4 as the raw materials. Briefly, 50 mg of CdS (g-C_3N_4) powder was dispersed in ethanol solution in a flask via ultrasound to form homogeneous CdS (g-C_3N_4) suspension. Then, a certain amount of 1T-MoS_{2+x} suspension was dropped into the CdS (g-C_3N_4) suspension under sonication for 30 min. Finally, the attained products were collected through filtering and dried at 55°C for 12 h under vacuum condition to obtain the 1T-MoS_{2+x}/CdS (1T-MoS_{2+x}/ g-C_3N_4) photocatalyst.

The photocatalytic test procedure of 1T-MoS_{2+x}/CdS and 1T-MoS_{2+x}/ g-C_3N_4 photocatalyst is similar to that of 1T-MoS_{2+x}/TiO_2 except for that 1T-MoS_{2+x}/CdS and 1T-MoS_{2+x}/g-C_3N_4 was irradiated via four illuminator with 420 nm. In addition, the sacrificial agent of 1T-MoS_{2+x}/CdS and 1T-MoS_{2+x}/g-C_3N_4 photocatalyst is 10% lactic acid solution and 10% methanol solution, respectively.

Figure captions

Fig. S1. The effect of Mo/S ratios on photocatalytic H_2-evolution rate of 1T-molybdenum sulfide-modified TiO_2(3%).

Fig. S2. XRD patterns of TiO_2 and 1T-MoS_{2+x}/TiO_2 photocatalysts.

Fig. S3. Band-gap evaluation from the plots of $(ahv)^2$ vs hv for various photocatalysts.

Fig. S4. Structure models of traditional 1T-MoS_2, 1T-MoS_{2+x}(V_{Mo}), 1T-MoS_{2+x}(S), and 1T-MoS_{2+x}(V_{Mo}+S) for DFT calculations (front, side, and top views).

Fig. S5. (a) Steady-state and (b) time-resolved photoluminescence spectra of (1) TiO_2, (2) 2H-MoS_2/TiO_2(5%), (3) 1T-MoS_2/TiO_2(5%), and (4) 1T-MoS_{2+x}/TiO_2(5%).

Fig. S6. (a) LSV curves, (b) transient photocurrent response, and (c) EIS spectra of various photocatalysts (R_{ctr} represents the charge-transfer resistance of the working electrode, R_{sr} represents the solution resistance (Na_2SO_4), and CPE represents the constant phase element between the electrolyte solution and electrode).

Table S1. Composition (at%) of the various samples according to XPS results

Sample	S	Mo	S/Mo
1T-MoS_2	57.43	42.57	1.35
1T-MoS_{2+x}	69.35	30.65	2.26

Table S2. The ICP-OES results (wt%) for various samples

Sample	S (wt%)	Mo (wt%)	Ti (wt%)	O (wt%)	Molar ratio of S/Mo	Actual mass ratio of 1T-MoS_{2+x}
1T-MoS_{2+x}/TiO_2(1%)	0.45	0.43	54.20	44.92	3.14	0.89
1T-MoS_{2+x}/TiO_2(5%)	2.19	2.13	53.21	42.47	3.08	4.52

Table S3. The H_2-evolution rate and apparent quantum efficiency (AQE) of various samples

samples	H_2-evolution rate (μmol h^{-1} g^{-1})	AQE (%)
TiO_2	10	0.03
2H-MoS_2/TiO_2(5.0%)	106	0.30
1T-MoS_2/TiO_2(5.0%)	321	0.91
1T-MoS_{2+x}/TiO_2(0.5%)	295	0.84
1T-MoS_{2+x}/TiO_2(1.0%)	577	1.64
1T-MoS_{2+x}/TiO_2(3.0%)	1381	3.93
1T-MoS_{2+x}/TiO_2(5.0%)	1624	4.62
1T-MoS_{2+x}/TiO_2(7.0%)	1095	3.11
1T-MoS_{2+x}/TiO_2(10%)	633	1.80

Table S4. Comparisons of photocatalytic H_2-evolution activity of TiO_2 modified with MoS_x-based cocatalysts

Photocatalyst	Sacrificial agent	Light source	Activity (μmol/h/g)/AQE	Ref.
1T-MoS_{2+x}/TiO_2	ethanol-water (25 vol%)	3 W LED 365 nm	1624	**This work**
MoS_2/TiO_2	ethanol-water (25 vol%)	3 W LED 365 nm	460	1
MoS_x/TiO_2	methanol-water	3 W LED 365 nm	1106	2
MoS_2@C/TiO_2	methanol-water (10 vol%)	3 W LED 365 nm	297	3
2H-MoS_2/TiO_2	methanol-water (0.1 M)	300 W Xe lamp	482	4
MoS_2-MoC@rGO/TiO_2	methanol-water (10 vol%)	3 W LED 365 nm	575	5
TiO_2@C/MoS_x	methanol-water (10 vol%)	3 W LED 365 nm	971	6
TiO_2-MoS_2(2H)	methanol-water (25 vol%)	300 W Xe lamp with 440 nm cut-off filter	250	7
a-MoS_x/TiO_2	lactic acid (10 vol%)	3 W LED 365 nm	3452	8
MoS_2/TiO_2(HPT)	0.35 M Na_2S and 0.25 M Na_2SO_3	300 W Xeon-lamp	1376	9
MoS_{2-x}@TiO_2-OV	Triethanolamine (20 vol%)	300 W Xeon-lamp	42	10
M-MoS_2/TiO_2(B)	methanol-water (20 vol%)	300 W Xeon-lamp	1444	11
MoS_2/TiO_2	methanol-water (20 vol%)	300 W Xeon-lamp with 420 nm cutoff filter	560	12

References

1. Q. Xiang, J. Yu and M. Jaroniec, *J. Am. Chem. Soc.*, 2012, **134**, 6575-6578.
2. H. Yu, R. Yuan, D. Gao, Y. Xu and J. Yu, *Chem. Eng. J.*, 2019, **375**, 121934.
3. J. Liu, P. Wang, L. Gao, X. Wang and H. Yu, *J. Mater. Chem. C*, 2022, **10**, 3121-3128.
4. H. Lin, K. Zhang, G. Yang, Y. Li, X. Liu, K. Chang, Y. Xuan and J. Ye, *Appl. Catal. B Environ.*, 2020, **279**, 119387.
5. M. Pan, L. Gao, P. Wang, X. Wang and H. Yu, *J. Alloys Compd.*, 2023, **939**, 168721.
6. J. He, W. Zhong, Y. Xu, J. Fan, H. Yu and J. Yu, *J. Mater. Chem. C*, 2021, **9**, 3239-3246.
7. S. Bai, L. Wang, X. Chen, J. Du and Y. Xiong, *Nano Res.*, 2015, **8**, 175-183.
8. D. Gao, R. Yuan, J. Fan, X. Hong and H. Yu, *J. Mater. Sci. Technol.*, 2020, 56, 122-132.
9. A. Tiwari, A. Gautam, S. Sk, D. S. Gavali, R. Thapa and U. Pal, *J. Phys. Chem. C*, 2021, **125**, 11950-11962.
10. Y. Wu, X. Chen, J. Cao, Y. Zhu, W. Yuan, Z. Hu, Z. Ao, G. W. Brudvig, F. Tian, J. C. Yu and C. Li, *Appl. Catal. B Environ.*, 2022, **303**, 120878.
11. J. Wang, H. Jia, Y. Guo, Y. Zhang, Q. Xie, H. Zhu, J. Sun, F. Shi, Z.-H. Liu and R. Jiang, *Solar RRL*, 2019, **3**, 1900323.
12. X. Liu, Z. Xing, H. Zhang, W. Wang, Y. Zhang, Z. Li, X. Wu, X. Yu and W. Zhou, *ChemSusChem*, 2016, **9**, 1118-1124.

Table S5. Fluorescence emission lifetime and relevant percentage data fitted by a three-exponential function

Samples	τ_1 (ns)	A_1 (%)	τ_2 (ns)	A_2 (%)	τ_3 (ns)	A_3 (%)	Average lifetime (τ_a) (ns)	χ^2
TiO_2	0.41	52.40	2.42	34.28	10.83	13.32	7.12	1.31
2H-MoS_2/TiO_2	0.40	49.96	2.99	36.61	13.14	13.43	8.67	1.17
1T-MoS_2/TiO_2	0.49	48.40	3.14	37.89	13.69	13.71	8.94	1.15
1T-MoS_{2+x}/TiO_2	0.41	49.07	3.04	38.44	14.19	12.49	9.16	1.13

The above fitted parameters are acquired via the following tri-exponential formulas:

$$I_{(t)} = I_0 + A_1\exp(-t/\tau_1) + A_2\exp(-t/\tau_2) + A_3\exp(-t/\tau_3) \qquad (1)$$

$$\tau_a = (A_1\tau_1^2 + A_2\tau_2^2 + A_3\tau_3^2)/(A_1\tau_1 + A_2\tau_2 + A_3\tau_3) \qquad (2)$$

where I_0 is the baseline correction value, A_1, A_2 and A_3 represent the tri-exponential factors, and τ_1, τ_2, τ_3 and τ_a corresponding the lifetime in various stages (radiation, non-radiation and energy transfer) and average lifetime, χ^2 is the goodness-of-fit.

Table S6. The fitted R_{sr} and R_{ctr} values from the EIS plots for various samples

Sample	R_{sr}(ohm)	R_{ctr}(ohm)
TiO_2	7.590	6.230E6
2H-MoS_2/TiO_2	7.846	3.056E6
1T-MoS_2/TiO_2	8.045	1.274E6
1T-MoS_{2+x}/TiO_2	7.282	4.091E5

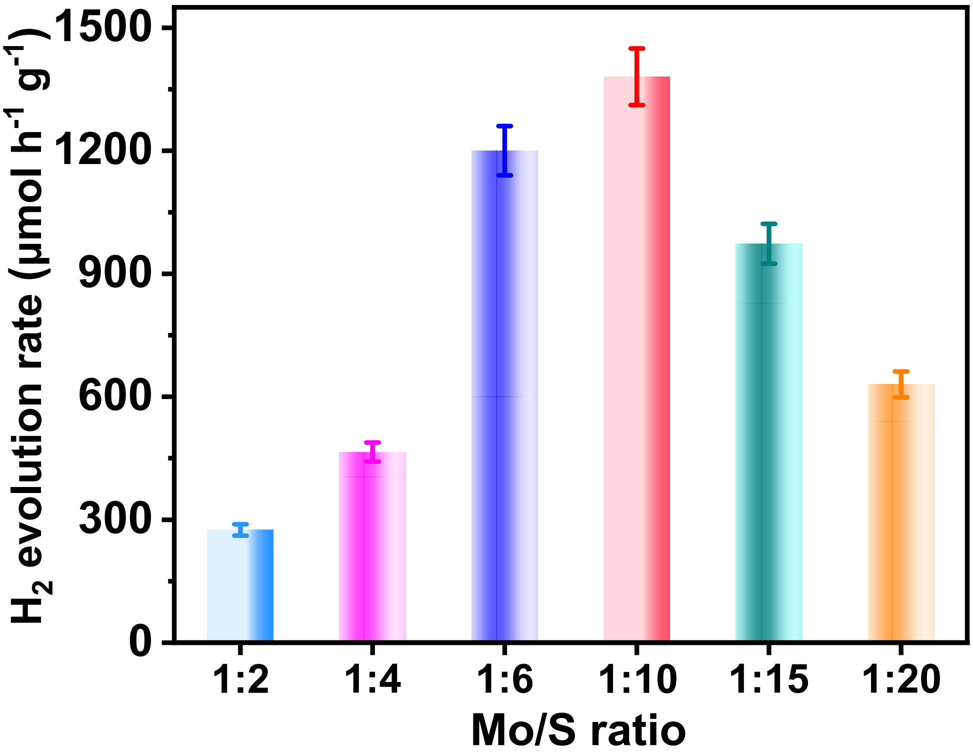

Fig. S1. The effect of Mo/S ratios on photocatalytic H_2-evolution rate of 1T-molybdenum sulfide-modified TiO_2(3%).

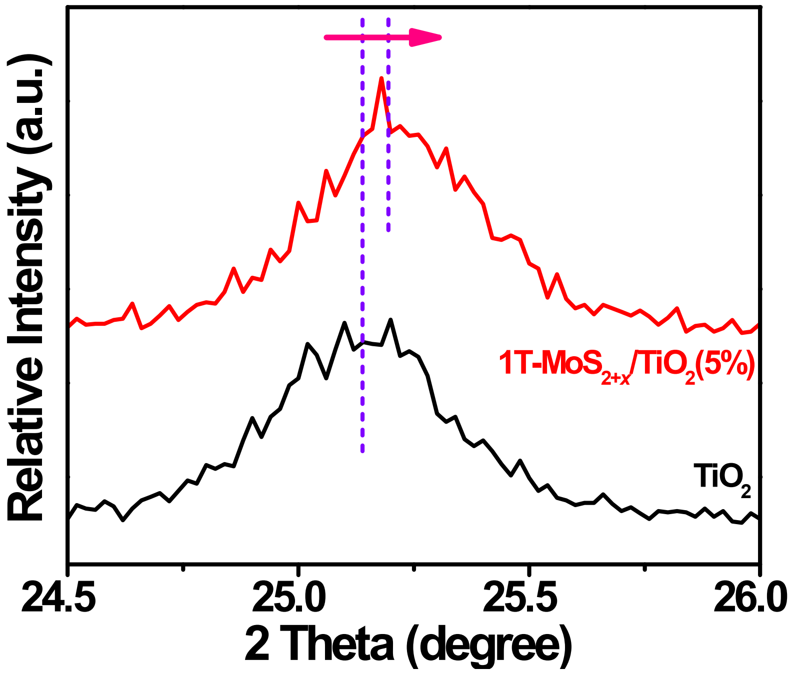

Fig. S2. XRD patterns of TiO$_2$ and 1T-MoS$_{2+x}$/TiO$_2$ photocatalysts.

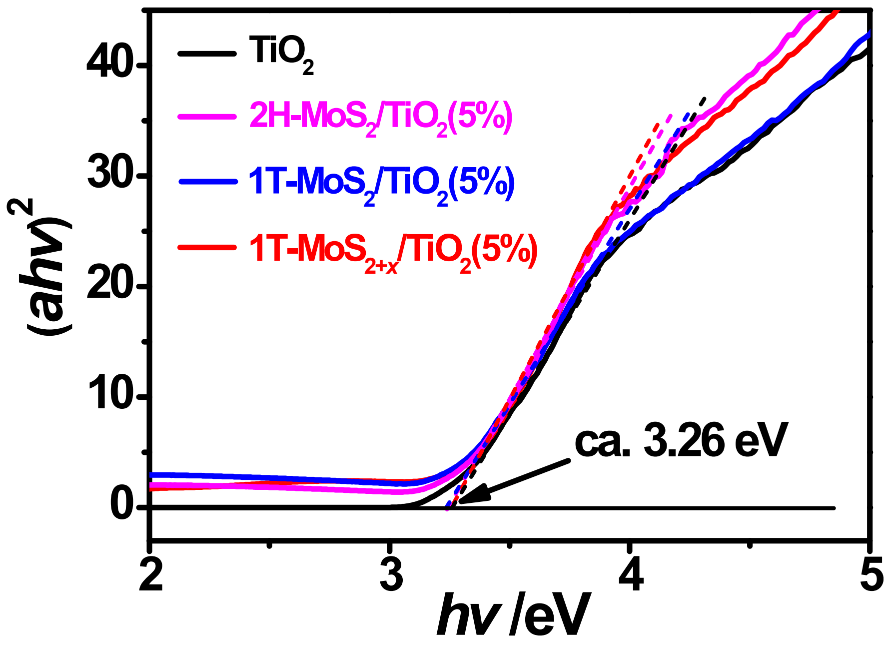

Fig. S3. Band-gap evaluation from the plots of $(ahv)^2$ vs hv for various photocatalysts.

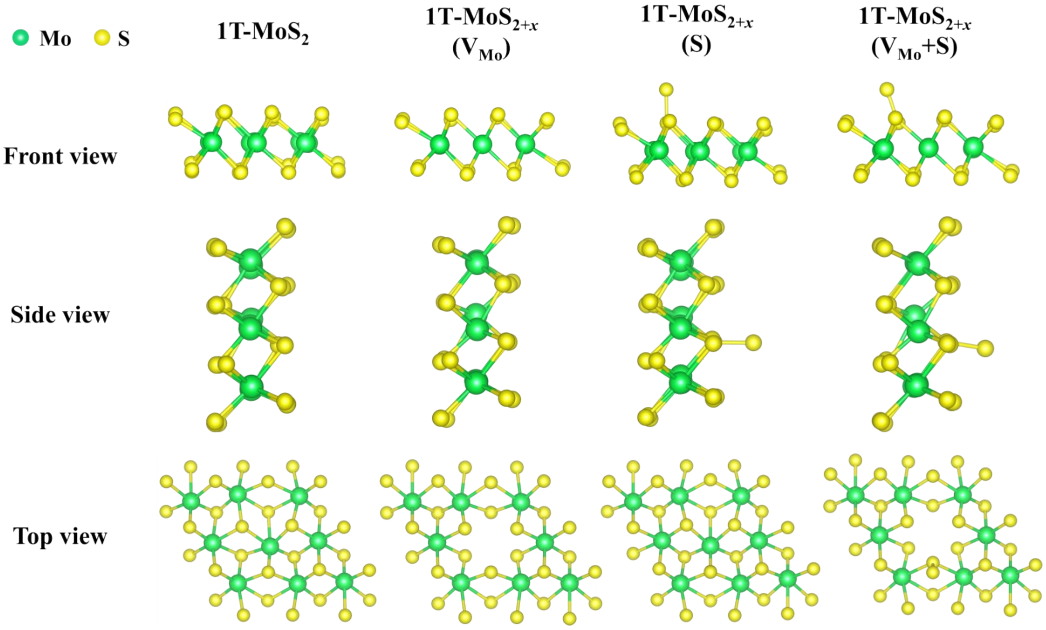

Fig. S4. Structure models of traditional 1T-MoS$_2$, 1T-MoS$_{2+x}$(V$_{Mo}$), 1T-MoS$_{2+x}$(S), and 1T-MoS$_{2+x}$(V$_{Mo}$+S) for DFT calculations (front, side, and top views).

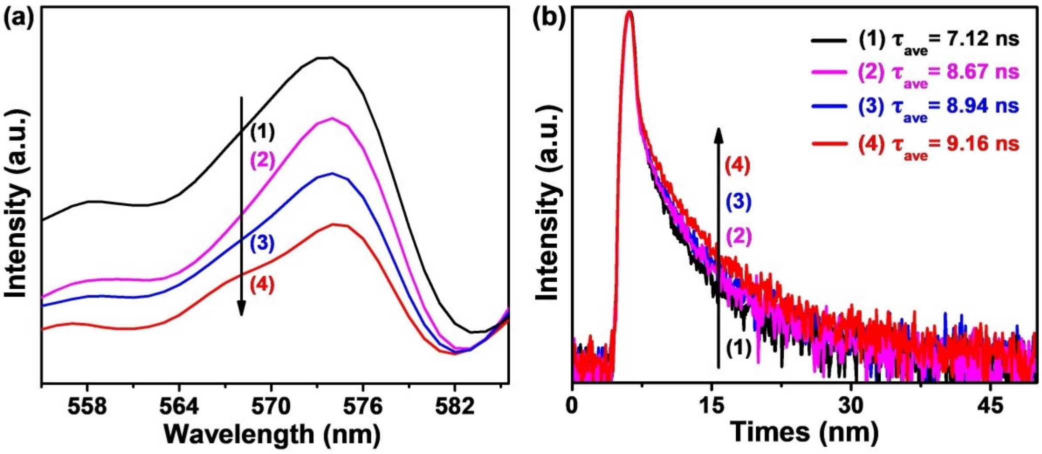

Fig. S5. (a) Steady-state and (b) time-resolved photoluminescence spectra of (1) TiO_2, (2) 2H-MoS_2/TiO_2(5%), (3) 1T-MoS_2/TiO_2(5%), and (4) 1T-MoS_{2+x}/TiO_2(5%).

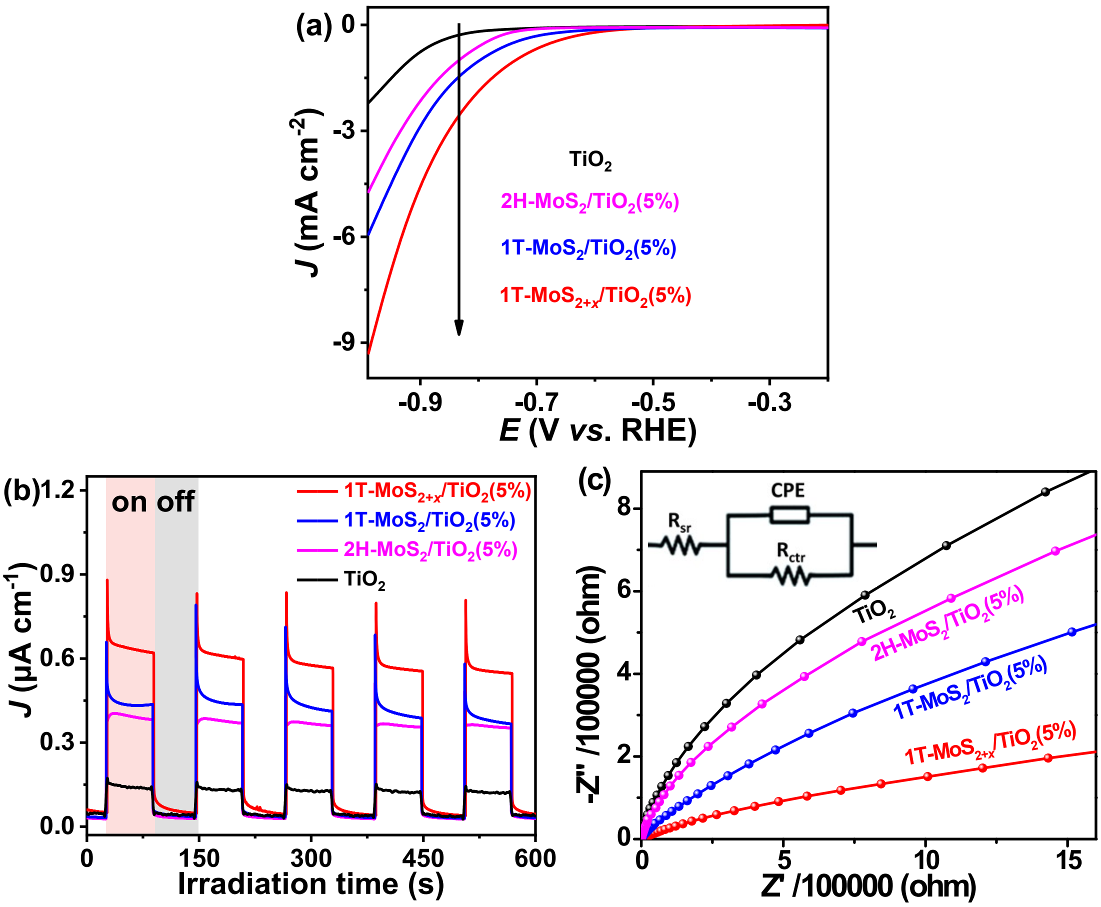

Fig. S6. (a) LSV curves, (b) transient photocurrent response, and (c) EIS spectra of various photocatalysts (R_{ctr} represents the charge-transfer resistance of the working electrode, R_{sr} represents the solution resistance (Na_2SO_4), and CPE represents the constant phase element between the electrolyte solution and electrode).